Optimally smooth symmetric quadrature mirror filters for image coding

Peter Niels Heller and Jerome M. Shapiro

Aware, Inc.
Cambridge, MA 02142

R. O. Wells, Jr.

Rice University
Houston, TX 77251

ABSTRACT

Symmetric quadrature mirror filters (QMF's) offer several advantages for wavelet-based image coding. Symmetry and odd-length contribute to efficient boundary handling and preservation of edge detail. Symmetric QMF's can be obtained by mildly relaxing the filter bank orthogonality conditions. We describe a computational algorithm for these filter banks which is also symmetric in the sense that the analysis and synthesis operations have identical implementations, up to a delay. The essence of a wavelet transform is its multiresolution decomposition, obtained by iterating the lowpass filter. This allows one to introduce a new design criterion, smoothness (good behavior) of the lowpass filter under iteration. This design constraint can be expressed solely in terms of the lowpass filter tap values (via the eigenvalue decomposition of a certain finite-dimensional matrix). Our innovation is to design near-orthogonal QMF's with linear-phase symmetry which are optimized for smoothness under iteration, not for stopband rejection. The new class of optimally smooth QMF filter banks yields high performance in a practical image compression system.

Keywords: wavelets, quadrature mirror filters, image coding, regularity

1 INTRODUCTION

The use of filter banks and wavelet decompositions is well-established for image coding. Iteration of the lowpass filter and good behavior of the resulting iterate play a key role in such multiresolution transforms. However, until recently, mechanisms did not exist to design filters which have optimal smoothness under iteration. We propose the Sobolev smoothness of the associated wavelet scaling function as a new filter design constraint which can be computed directly from the lowpass filter taps. We apply this design constraint to odd-length symmetric quadrature mirror filter (QMF) pairs. In order to obtain symmetry of the two-channel filter QMF bank, the orthogonality constraints must be mildly relaxed.

This paper is organized as follows: Section 2 reviews the construction of symmetric (linear-phase) quadrature mirror filters, and their advantages for image coding. Section 3 describes an efficient implementation of these filter banks, in which the analysis and synthesis stages have effectively identical implementations. Section 4 reviews the theory of wavelet bases and their regularity (differentiability). Section 5 introduces Sobolev smoothness of the infinite iterate as a new filter design constraint, and applies this as a criterion to construct a new class of symmetric QMF's. In Section 6 we apply the new filter banks to the compression of a variety of images, and compare their performance with previously known 2-channel filter banks.

2 QUADRATURE MIRROR FILTERS FOR IMAGE CODING

Quadrature mirror filters (QMF's) are two-channel filter banks in which the highpass filter is obtained by an "alternating flip" of the lowpass filter. If the lowpass filter of the pair is $h_0[n]$, a sequence of length N, then the highpass filter is given by

$$h_1[n] = (-1)^n h_0[N-1-n] \ . \tag{1}$$

This can be represented in the frequency domain as

$$H_1(\omega) = e^{i\omega} H_0(\pi - \omega) \ ;$$

H_1 is a "mirror" of H_0. One often combines this construction with orthogonality of the filter bank,

$$\sum_n h_0[n] h_0[n+2l] = \delta_{0,l} \tag{2}$$

to assure perfect reconstruction overall. It was shown rather early in the theory of multirate filter banks[16,18] that the only symmetric two-channel orthogonal QMF pair is the Haar filter, for which $h_0 = \{1, 1\}$. This filter is too crude for most image coding applications. However, symmetry (linear-phase) for filter banks is an important property in wavelet and subband image coders; it enables the use of nonexpansive symmetric extension methods at signal boundaries.[14] One solution to this problem is to give up the QMF condition and seek filter banks which are perfect-reconstruction (biorthogonal), rather than paraunitary (orthogonal).[2,12,19] This approach led to the well-known (7,9)-tap biorthogonal wavelet pair used in the FBI's fingerprint compression standard.

A different solution to the problem of symmetry and orthogonality was developed by Adelson and Simoncelli[1]; they *mildly relaxed* the orthogonality condition (2) and by doing so were able to obtain symmetric filters! The odd-length filters they designed satisfied the orthogonality conditions (2) within 1.0e-3, and led to near-perfect-reconstruction of wavelet-transformed images. The use of odd-length filters is also noteworthy, for the whole-sample symmetry of an odd-length filter preserves centers of mass, leading to better retention of edge details in a lossy subband compression scheme. Even-length filters will smear single-pixel detail across two filter outputs, leading to smoothed, blurry artifacts. Further constructions of these near-perfect-reconstruction QMF's[7] have been based on traditional filter design constraints such as stopband attenuation.

3 COMPUTATIONAL ADVANTAGES OF SYMMETRIC QMF'S

Symmetric odd-length QMF's posess an elegant computational scheme which employs the same basic algorithm for computing the analysis and synthesis transforms. This leads to flexibility and reusability of software and hardware which is not possible with most filterbanks; usually the analysis and synthesis (or encode and decode) operations require distinct implementations. We now develop the flexible implementation.

In the symmetric case, the QMF relationship (1) becomes

$$h_1[n] = (-1)^n h_0[n] \tag{3}$$

Now, in the application of the filters on the data for the 2-channel filterbank, the lowpass output is sampled on the even phases and the highpass filter is sampled on the odd phases. Consider the output of the lowpass filter and downsampler to be

$$x_l[n] = \sum_{k=0}^{N-1} h_0[k]x[n-k]\frac{1+(-1)^n}{2} \tag{4}$$

and the output of the highpass filter and downsampler as

$$\begin{aligned} x_h[n] &= \sum_{k=0}^{N-1} h_1[k]x[n-k]\frac{1-(-1)^n}{2} &(5)\\ &= \sum_{k=0}^{N-1} h_0[k]x[n-k]\frac{(-1)^k-(-1)^{n+k}}{2}. &(6)\end{aligned}$$

Notice that we are maintaining the sampling rate of the original signals, and the downsampler merely sets the odd samples to zero for the lowpass case, and the even samples to zero for the highpass case.

If we define a composite signal $y[n] = x_l[n] + x_h[n]$, then

$$y[n] = \sum_{k=0}^{N-1} h_0[k]x[n-k]\frac{1+(-1)^n+(-1)^k-(-1)^{n+k}}{2} \tag{7}$$

Essentially, the composite signal alternates between low pass and high pass outputs. We want to consider two different reconstruction methods and show they are identical.

The usual reconstruction process is accomplished by convolving $x_l[n]$ with $h_0[n]$, convolving $x_h[n]$ with $h_1[n]$ and adding the results. Denoting the reconstructed signal by $u[n]$,

$$\begin{aligned} u[n] &= \sum_{k=0}^{N-1} h_0[k]x_l[n-k] + h_1[k]x_h[n-k] &(8)\\ &= \sum_{k=0}^{N-1} h_0[k](x_l[n-k] + (-1)^k x_h[n-k]) &(9)\end{aligned}$$

Now consider defining the signals $y_e[n]$, and $y_o[n]$ which are the output of the two channel filterbank applied to $y[n]$, but sampling the highpass output on the even phases and the lowpass output on the odd phases. We have

$$\begin{aligned} y_e[n] &= \sum_{k=0}^{N-1} h_1[k]y[n-k]\frac{1+(-1)^n}{2} &(10)\\ &= \sum_{k=0}^{N-1} h_1[k](x_l[n-k]+x_h[n-k])\frac{1+(-1)^n}{2} &(11)\end{aligned}$$

and

$$y_o[n] = \sum_{k=0}^{N-1} h_0[k] y[n-k] \frac{1-(-1)^n}{2} \tag{12}$$

$$= \sum_{k=0}^{N-1} h_0[k](x_l[n-k] + x_h[n-k]) \frac{1-(-1)^n}{2}. \tag{13}$$

Adding the two together, we define

$$v[n] = y_e[n] + y_o[n] \tag{14}$$

$$= \sum_{k=0}^{N-1} x_l[n-k] \left(h_0[k] \frac{1-(-1)^n}{2} + h_1[k] \frac{1+(-1)^n}{2} \right) + \tag{15}$$

$$x_h[n-k] \left(h_0[k] \frac{1-(-1)^n}{2} + h_1[k] \frac{1+(-1)^n}{2} \right). \tag{16}$$

Now $x_l[n-k]$ is non-zero only when n and k are either both even or both odd, so $(-1)^n = (-1)^k$. Similarly, $x_h[n-k]$ is non-zero when $(-1)^n = -(-1)^k$. Substituting in, we have

$$v[n] = \sum_{k=0}^{N-1} x_l[n-k] \left(h_0[k] \frac{1-(-1)^k}{2} + h_1[k] \frac{1+(-1)^k}{2} \right) + \tag{17}$$

$$x_h[n-k] \left(h_0[k] \frac{1+(-1)^k}{2} + h_1[k] \frac{1-(-1)^k}{2} \right) \tag{18}$$

$$= \sum_{k=0}^{N-1} h_0[k] x_l[n-k] + (-1)^k x_h[n-k]], \tag{19}$$

which is the same as (9), and therefore $v[n] = u[n]$.

Thus, when using symmetric QMF filters, the structure used to compute the analysis is identical to the structure used to compute the synthesis, except for a shift by one sample. Using local memory to store partial results, the computational cost is 8 adds and 5 multiplies per output point; one can reduce this further when the QMF has one or more vanishing moments as discussed below. This leads to an operation count similar to that of the Daubechies (7,9)-tap pair.[2]

4 WAVELET BASES AND REGULARITY

We review now some fundamentals of discrete and continuous wavelet bases, and the notion of their smoothness or regularity. The dyadic wavelet transform or multiresolution analysis is formed by iterating a two-channel filterbank. The resulting octave-band decomposition has proven especially useful for image coding both because it yields superior energy compaction and because it is well-matched to the human visual system.[11] The frequency response of a lowpass filter iterated K times (omitting aliasing terms) is

$$H^K(\omega) = \prod_{j=1}^{K} H_0(\omega/2^j). \tag{20}$$

When designing FIR lowpass filters for use in such a discrete wavelet transform, it is appropriate to consider the filter's behavior under iteration. This was first done by Daubechies[4] in the course of constructing continuous-time compactly supported orthonormal wavelet bases.

The continuous-time wavelet basis is determined by the scaling function, which is the solution to the dilation equation

$$\phi(x) = \sum_n h_0[n]\phi(2x-n) \tag{21}$$

where the $h_0[n]$ are the taps of the lowpass filter in the wavelet filter bank. From the Fourier transform point of view, $\hat{\phi}$ is the result of taking the infinite limit of the iteration (20):

$$\hat{\phi}(\omega) = \prod_{j=1}^{\infty} H_0(\omega/2^j) \ .$$

These equations have well-defined solutions whether or not the function ϕ leads to a true orthonormal wavelet basis;[3,6] thus it makes sense to speak of the scaling function in the case of the near-orthogonal QMF's under study here.

4.1 Regularity for wavelet systems

The smoothness of continuous-time wavelet systems has been the object of intensive study.[4,6,8,10,20,21] Because the wavelet $\psi(x)$ is determined from the scaling function by means of the highpass filter taps

$$\psi(x) = \sum_n h_1[n]\phi(2x-n) \ ,$$

it is the smoothness of the scaling function (infinitely iterated lowpass filter) which determines the smoothness of the overall wavelet system.

Daubechies' construction[4] imposed N vanishing wavelet moments

$$\int x^k \psi(x)dx = 0 \quad k = 0, 1, \ldots, N-1$$

as a means of ensuring smoothness; this condition is equivalent to an N-th order zero at π for the lowpass filter:

$$\sum_n (-1)^n n^k h_0[n] = 0 \quad k = 0, 1, \ldots, N-1 \ . \tag{22}$$

This condition was motivated by a theorem[5] which states that if an orthonormal system of dilates and translates

$$\left\{ 2^{j/2}\psi(2^j x - k) \right\}$$

is made up of N times continuously differentiable functions, then the generating wavelet $\psi(x)$ must have N vanishing moments.

In the case of the odd-length symmetric QMF's, we have the following

Proposition: If the filter h_0 is odd-length, symmetric, and its frequency response $H_0(\omega)$ has a first order zero at π, then $H_0(\omega)$ has a second-order zero at π.

Proof: We prove this in the case where the filter h_0 has length $4L+1$; the proof for length $4L+3$ is similar. Given that h_0 is symmetric of length $4L+1$ and H_0 has a first order zero at π, equation (22) becomes

$$h[2L] + 2\sum_{n=0}^{2L-1} (-1)^n h_0[n] = 0 \ .$$

Thus

$$h[2L] + 2\sum_{n=0}^{L-1} h_0[2n] = 2\sum_{n=0}^{L-1} h_0[2n+1]\ .$$

We can multiply this equation by $2L$ to get

$$2Lh[2L] + 4L\sum_{n=0}^{L-1} h_0[2n] = 4L\sum_{n=0}^{L-1} h_0[2n+1]\ .$$

Breaking each $4L$ into $2n$ and $4L-2n$, we can rearrange this into

$$\sum_{n=0}^{4l} (-1)^n n h_0[n] = 0\ .$$

Thus the filter $H_0(\omega)$ has a second order zero at π. ∎

In her original paper, Daubechies showed that the N-vanishing-moment construction led to scaling functions of arbitrary differentiability, if N is taken large enough. In the meantime, several authors[3,6,8,10,20,21] have developed refined tools for measuring the smoothness (differentiability) of solutions to dilation equations such as (21). This study requires a set of function spaces which include the usual classes $\mathcal{C}^N$ of N-times continuously differentiable functions, and interpolates between them. This is usually done with Hölder (also known as Lipschitz) or Sobolev notions of differentiability. We will use the Sobolev, or L^2 notion here.

Given a real number s, the Sobolev space $\mathcal{H}^s$ is defined by

$$\mathcal{H}^s := \left\{ f\ :\ \|f\|^2_{\mathcal{H}^s} = \int_{\mathbf{R}} |\hat{f}(\omega)|^2 \left(1+|\omega|^2\right)^s d\omega < \infty \right\}\ .$$

Recall that for $f : \mathbf{R} \to \mathbf{C}$, $f \in \mathcal{H}^s \Rightarrow f \in \mathcal{C}^\alpha$, for $\alpha < s - \frac{1}{2}$. That is, if $s > n + \frac{1}{2}$, then f has n continuous derivatives. We define the *Sobolev smoothness* of a function $\phi \in L^2(\mathbf{R})$ to be

$$s(\phi) := \sup\left\{ s\ :\ \phi \in \mathcal{H}^s \right\}\ .$$

It has been shown[8,20] that when ϕ is the solution to a dilation equation (21), the Sobolev smoothness of ϕ is determined by the maximum eigenvalue of a finite-dimensional operator associated with the coefficient sequence $h_0[n]$. In particular, consider the modulus squared of the lowpass frequency response, denoted by P:

$$P(\omega) = |H_0(\omega)|^2\ ,$$

and the associated "multiresolution operator" or "transition operator" which takes functions on $[0,\pi)$ to functions on $[0,\pi)$:

$$T_P u(\omega) \quad = \quad P\left(\frac{\omega}{2}\right) u\left(\frac{\omega}{2}\right) + P\left(\frac{\omega+2\pi}{2}\right) u\left(\frac{\omega+2\pi}{2}\right)\ .$$

T_P is defined in the time domain as the operator taking a sequence u_n to

$$(\check{T_P} u)_n = m\sum_{k,l} h_0[k]\overline{h_0[l]} u_{2n+k-l}\ . \tag{23}$$

Let the trigonometric polynomial P be given as in (4.1), expressed in the form

$$P(e^{i\omega}) = \sum_{j=-J}^{J} p_j e^{ij\omega}\ . \tag{24}$$

Moreover define the $2J+1$-dimensional space of trigonometric polynomials

$$\mathcal{E}_J := \left\{ u(\omega) = \sum_{j=-J}^{J} u_j e^{ij\omega} \right\} ,$$

as well as the distinguished subspace

$$\mathcal{F}_{J,N} := \left\{ f \in \mathcal{E}_J : f(\omega) = (1-\cos\omega)^N g(\omega) \right\} .$$

We know the following:[5,8,20]

THEOREM 4.1. *Suppose that the wavelet system associated with the lowpass filter $\{h_0[n]\}$ has N vanishing wavelet moments. Then*

(i) *The subspace $\mathcal{E}_J$ of $\mathcal{C}[0,\pi]$ is an invariant subspace for the operator T_P, i.e.*

$$T_P : \mathcal{E}_J \rightarrow \mathcal{E}_J .$$

The operator T_P acting on $\mathcal{E}_J$ has the matrix representation $t_{j,k} = p_{2j-k}$, or

$$T = \begin{bmatrix} p_J & 0 & 0 & 0 & \dots & 0 & 0 \\ p_{J-2} & p_{J-1} & p_J & 0 & \dots & 0 & 0 \\ & & \ddots & & & & \\ p_J & p_{J-1} & p_{J-2} & \dots & p_{J-2} & p_{J-1} & p_J \\ 0 & 0 & p_J & \dots & p_{J-4} & p_{J-3} & p_{J-2} \\ & & & & \ddots & & \\ 0 & 0 & 0 & \dots & p_J & p_{J-1} & p_{J-2} \\ 0 & 0 & 0 & \dots & 0 & 0 & p_J \end{bmatrix}$$

with respect to the basis $\left\{e^{-iJ\omega}, \dots, 1, \dots, e^{iJ\omega}\right\}$.

(ii) *$T_P|_{\mathcal{E}_J}$ has eigenvalues 2^{-n}, $n = 0, 1, \dots, 2N-1$. Furthermore, the eigenvectors corresponding to these eigenvalues lie in $\mathcal{F}_{J,N}^{\perp}$.*

(iii) *If μ is the largest eigenvalue of $T_P|_{\mathcal{F}_{J,N}}$ and $\mu < \frac{1}{2}$,*

$$s(\phi) = -\frac{\log\mu}{2\log 2} . \tag{25}$$

Thus we have obtained an explicit formula for the Sobolev smoothness of the scaling function ϕ in terms of the maximal eigenvalue of the associated multiresolution operator T_P acting on a distinguished subspace of the finite-dimensional space $\mathcal{E}_{N-1}$.

5 A SMOOTHNESS CRITERION FOR WAVELET FILTER DESIGN

The results of the previous section give us a new filter design criterion – we can design FIR lowpass filters which lead to maximally smooth scaling functions (infinitely iterated lowpass filters). Since the smoothness of finite iterates of the lowpass filter qualitatively corresponds to the smoothness of the scaling function,[13] we can use the mathematical tools developed for the continuous-time setting to help us design wavelet filters with smooth finite iterates. This is important for wavelet-based image coding because the artifacts resulting from the lossy step of quantization reflect the shape of the underlying basis function. If we can optimize the smoothness of the discrete wavelet basis functions resulting from iteration of the lowpass filter, then we should achieve superior perceptual quality for images compressed using these maximally smooth wavelets. Our algorithm for measuring the smoothness of a given lowpass filter is the following:

- Form the deterministic autocorrelation sequence $p[j]$ and the matrix of Theorem 4.1.
- Find the maximal eigenvalue of this matrix, other than the sequence 2^{-n}, $n = 0, 1, \ldots, 2N-1$.
- The Sobolev smoothness (number of L^2 derivatives) of the scaling function associated to the lowpass filter is
$$s(\phi) = -\frac{\log \mu}{2 \log 2} .$$

5.1 Design of Sobolev-optimal QMF's

We now apply our Sobolev-optimality criterion to the design of symmetric near-orthogonal QMF's. We impose several constraints on the filters: we constrain the length:

$$\sum_n h_n^2 = 1 \ , \tag{26}$$

and we impose one (and therefore two) vanishing wavelet moments:

$$\sum_n h_n = \sqrt{2} \ , \tag{27}$$

$$\sum_n (-1)^n h_n = 0 \ . \tag{28}$$

Observe that if the filters were truly orthogonal (i.e. fully satisfied the conditions (2)), then one of the equations (27)-(28) would be superfluous. However, in the near-orthogonal case of symmetric QMF's, both equations are necessary. This leaves two free parameters for a nine-tap QMF (one parameter for the seven-tap case). We optimized to find the filter with the greatest Sobolev smoothness while satisfying the orthogonality constraints (2) to within a reasonable epsilon (less than 1e-03). This amounts to the nonlinearly constrained optimization problem of finding the solution which minimizes the deviation from orthogonality while maximizing the Sobolev exponent. We obtained this minimax solution by a search of the two-parameter space; deeper mathematical analysis of the saddle point behavior is in order.

This approach yields a new family of QMFs; the 7- and 9-tap examples are given in Table 1 below. The 9-tap Sobolev-optimal QMF is quite distinct from the 9-tap QMF of Adelson-Simoncelli[1]; its frequency response is plotted in Figure 1, while pictures comparing the corresponding scaling and wavelet functions are shown in Figure 2. Observe that our Sobolev-optimal design yielded a flatter frequency response than the frequency-sampling approach.[1] The scaling function associated with the Sobolev-optimal QMF has Sobolev exponent $s = 1.795$, and is visibly smoother than the scaling function associated with the Adelson-Simoncelli QMF, which has $s = 1.567$. Both of these scaling functions are smoother than the analysis scaling function of the Daubechies (7,9)-tap pair, which has $s = 1.410$. The Sobolev-optimal 9-tap QMF has a maximum deviation from orthogonality of $6.6e-04$, superior to the $7.9e-04$ max deviation for the Adelson-Simoncelli 9-tap QMF. The new 7-tap Sobolev-optimal QMF proved to be quite similar to Adelson and Simoncelli's 7-tap design.

n	$h_0[n]$	n	$h_0[n]$
0	-7.8125000e-03	0	1.9531250e-02
1	-7.3069675e-02	1	-4.6875000e-02
2	3.6136589e-01	2	-7.3234012e-02
3	8.5324613e-01	3	4.0042839e-01
		4	8.1451231e-01

Table 1: 7 and 9-tap Sobolev-optimal QMF lowpass filters.

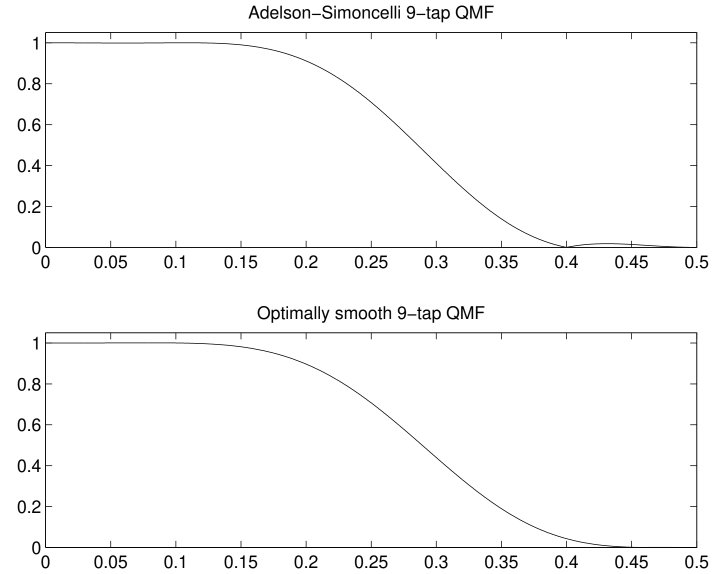

Figure 1: Frequency responses of Adelson-Simoncelli and optimally smooth lowpass filters.

6 IMAGE CODING RESULTS

We applied the new QMF banks to lossy wavelet-based image compression of natural and fingerprint images. After performing a wavelet transform, we applied entropy-constrained scalar quantization and Huffman coding to the transform coefficients. We used Mallat's wavelet tree[11] for compressing the NITF6 (Lenna) and NITF7 (aerial photography) images, and the FBI's Wavelet Scalar Quantization specified tree[9] to compare a fingerprint image. The results are shown in Tables 2, 2, and 4. All three filter banks used (Daubechies (7,9), Adelson-Simoncelli QMF, and Sobolev-optimal QMF) performed similarly, with a slight advantage in pSNR for the Daubechies (7,9)-tap pair. However, when compressing the fingerprint image, the (7,9)-tap pair produced artifacts at 32:1 not noticeable in either of the QMF-compressed images. We believe that the flat frequency response of the Sobolev-optimal filters will prove useful for compressing images with a wide range of frequency responses, such as a "zone plate."

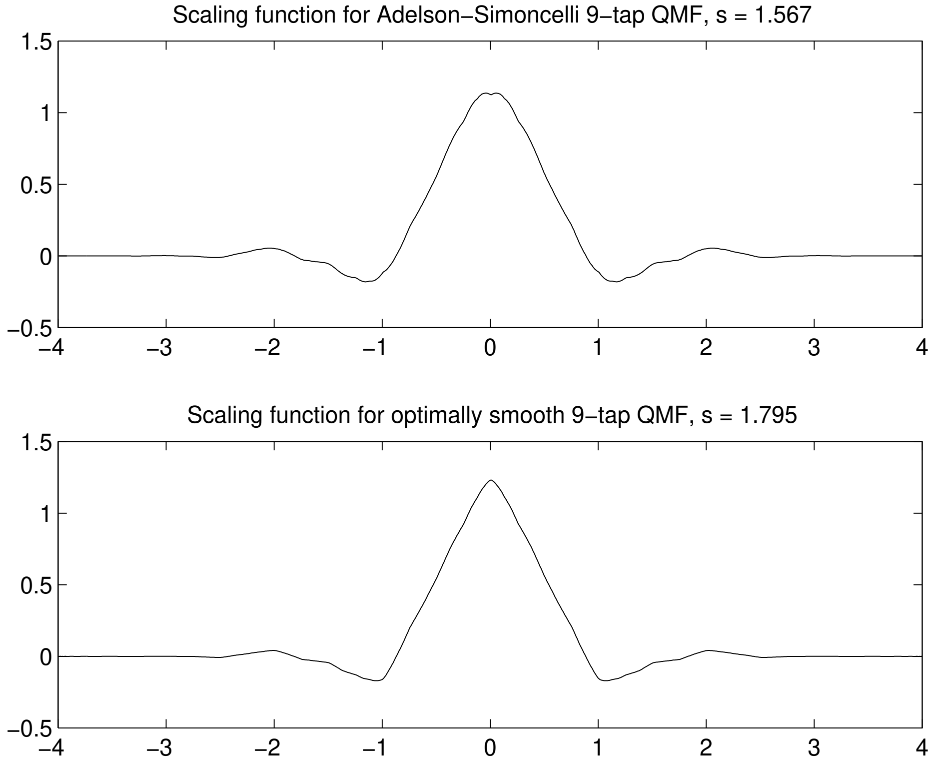

Figure 2: Comparison of Adelson-Simoncelli and optimally smooth scaling functions.

7 Acknowledgements

This research was supported in part by the Advanced Research Projects Agency of the Department of Defense and was monitored by the Air Force Office of Scientific Research under contract no. F49620-92-C-0054.

	8:1		16:1		32:1	
Filter	pSNR	Max	pSNR	Max	pSNR	Max
Daubechies (7,9)	37.99	28	35.06	42	31.96	58
Adelson-Simoncelli QMF	37.80	28	34.81	42	31.59	58
Sobolev-optimal QMF	37.79	28	34.74	44	31.48	61

Table 2: Peak SNR and maximum errors for compression of *Lenna* (Mallat tree, Daubechies (7,9)-tap pair, A-S QMF, and Sobolev-optimal QMF).

	8:1		16:1		32:1	
Filter	pSNR	Max	pSNR	Max	pSNR	Max
Daubechies (7,9)	24.79	126	21.63	148	19.55	218
Adelson-Simoncelli QMF	24.68	128	21.49	158	19.50	218
Sobolev-optimal QMF	24.68	111	21.49	152	19.47	220

Table 3: Peak SNR and maximum errors for compression of NITF7 aerial image (Mallat tree, Daubechies (7,9)-tap pair, A-S QMF, and Sobolev-optimal QMF).

	8:1		16:1		32:1	
Filter	pSNR	Max	pSNR	Max	pSNR	Max
Daubechies (7,9)	36.45	18	31.92	38	28.42	88
Adelson-Simoncelli QMF	36.35	18	31.87	36	28.53	78
Sobolev-optimal QMF	36.06	19	31.67	34	28.40	86

Table 4: Peak SNR and maximum errors for compression of fingerprint image (WSQ tree, Daubechies (7,9)-tap pair, A-S QMF, and Sobolev-optimal QMF).

8 REFERENCES

[1] E. Adelson, E. Simoncelli, and R. Hingorani, "Orthogonal Pyramid Transforms for image coding," in *Proc. SPIE Visual Commun. and Image Proc. II,* Cambridge, MA 1987.

[2] M. Antonini, M. Barlaud, P. Mathieu, and I. Daubechies, "Image Coding Using the Wavelet Transform," *IEEE Trans. on Image Processing,* 1 (1992), pp. 205-220.

[3] A. Cavaretta, W. Dahmen, and C. Micchelli, *Stationary Subdivision,*, Mem. Amer. Math. Soc., 453 (1991).

[4] I. Daubechies, "Orthonormal bases of compactly supported wavelets," *Comm. Pure Appl. Math.,* 41 (1988), pp. 909-996.

[5] I. Daubechies, *Ten Lectures on Wavelets*, CBMS Conference Series 61, SIAM, Philadelphia, 1992.

[6] I. Daubechies and J. Lagarias, "Two-scale difference equations I. Existence and global regularity of solutions," *SIAM J. Math. Anal.*, 22 (1991), pp. 1388-1410.

[7] A. Divakaran and W. Pearlman, "A Closed form expression for an efficient class of quadrature mirror filters and its FIR approximation," submitted to *IEEE Trans. on Circuits and Systems, part II*, 1992.

[8] T. Eirola, "Sobolev characterization of solutions of dilation equations," *SIAM J. Math. Anal.,* 23 (1992), pp. 1015-1030.

[9] Fed. Bureau of Investig., *WSQ Gray-Scale Fingerprint Image Compression Specification,* IAFIS-IC-0110-v2, Feb. 1993. Drafted by T. Hopper, C. Brislawn, and J. Bradley.

[10] P. N. Heller and R. O. Wells, Jr., "The Spectral Theory of Multiresolution Operators and Applications," in *Wavelets: Theory, Algorithms, and Applications,* C. K. Chui, L. Montefusco, L. Puccio, eds., Academic Press, San Diego, 1994, pp. 13-31.

[11] S. Mallat, "A Theory for multiresolution signal decomposition: the wavelet representation," *IEEE Trans. PAMI,* 11 (1989), pp. 674-693.

[12] T. Q. Nguyen and P. P. Vaidyanathan, "Two-Channel Perfect-Reconstruction FIR QMF Structures Which Yield Linear-Phase Analysis and Synthesis Filters," *IEEE Trans. on ASSP,* 37 (1989), pp. 676-690.

[13] O. Rioul and M. Vetterli, "Wavelets and signal processing," *IEEE SP Magazine,* vol. 8, no. 3 (1991), pp. 14-38.

[14] M. J. T. Smith and S. Eddins, "Analysis-synthesis techniques for subband image coding," *IEEE Trans. ASSP,* 38 (1990), pp. 1446-1456.

[15] P. Steffen, P. N. Heller, R. A. Gopinath, C. S. Burrus, "Theory of Regular M-band Wavelets," *IEEE Trans. on SP,* 41 (1993), pp. 3497-3511.

[16] M. J. T Smith and T. P. Barnwell III, "Exact Reconstruction Techniques for Tree-Structured Subband Coders," *IEEE Trans. on ASSP,* 34 (1986), pp. 434-441.

[17] G. Strang, "Wavelets and dilation equations," *SIAM Review,* 31 (1989), pp. 614-627.

[18] P. P. Vaidyanathan, *Multirate Systems and Filter Banks*, Prentice-Hall, Englewood Cliffs, NJ, 1992.

[19] M. Vetterli and C. Herley, "Wavelets and Filter Banks," *IEEE Trans. on SP*, 40 (1992), pp.2207-2233.

[20] L. Villemoes, "Energy moments in time and frequency for two-scale difference equation solutions and wavelets," *SIAM J. Math. Anal.,* 23 (1992), pp. 1519-1543.

[21] H. Volkmer, "On the regularity of wavelets," *IEEE Trans. on Info. Theory,* 38 (1992), pp. 872-876.